

---

---

# Complementary Roles of $^{18}\text{F}$ -DOPA PET/CT and $^{18}\text{F}$ -FDG PET/CT in Medullary Thyroid Cancer

Saila Kauhanen<sup>\*1,2</sup>, Camilla Schalin-Jäntti<sup>\*3</sup>, Marko Seppänen<sup>1,4</sup>, Sami Kajander<sup>1</sup>, Sami Virtanen<sup>5</sup>, Jukka Schildt<sup>6</sup>, Irina Lisinen<sup>1</sup>, Aapo Ahonen<sup>6</sup>, Ilkka Heiskanen<sup>7</sup>, Mika Väisänen<sup>7</sup>, Johanna Arola<sup>8,9</sup>, Pirkko Korsoff<sup>10</sup>, Tapani Ebeling<sup>11</sup>, Timo Sane<sup>3</sup>, Heikki Minn<sup>1,12</sup>, Matti J. Välimäki<sup>3</sup>, and Pirjo Nuutila<sup>1,13</sup>

<sup>1</sup>Turku PET Centre, Turku University Hospital, Turku, Finland; <sup>2</sup>Department of Surgery, Turku University Hospital, Turku, Finland; <sup>3</sup>Department of Medicine, Division of Endocrinology, Helsinki University Hospital, Helsinki, Finland; <sup>4</sup>Department of Nuclear Medicine, Turku University Hospital, Turku, Finland; <sup>5</sup>Medical Imaging Centre of Southwest Finland, Turku, Finland; <sup>6</sup>Helsinki PET Centre, Helsinki University Hospital, Helsinki, Finland; <sup>7</sup>Department of Surgery, Helsinki University Hospital, Helsinki, Finland; <sup>8</sup>Department of Pathology, Haartman Institute, University of Helsinki, Helsinki, Finland; <sup>9</sup>HUSLAB, Helsinki University Hospital, Helsinki, Finland; <sup>10</sup>Department of Medicine, Satakunta Central Hospital, Pori, Finland; <sup>11</sup>Department of Medicine, Oulu University Hospital, Oulu, Finland; <sup>12</sup>Department of Oncology and Radiotherapy, Turku University Hospital, Turku, Finland; and <sup>13</sup>Department of Medicine, University of Turku, Turku, Finland

Serum calcitonin and carcinoembryonic antigen (CEA) are markers of recurrent or persistent disease in medullary thyroid cancer (MTC). However, conventional imaging often fails to localize metastatic disease. Our aim was to compare fluorine-labeled dihydroxyphenylalanine ( $^{18}\text{F}$ -DOPA) and  $^{18}\text{F}$ -FDG PET/CT with multidetector CT (MDCT) and MRI in recurrent or persistent MTC. **Methods:** Nineteen MTC patients with increased calcitonin or CEA on follow-up (mean  $\pm$  SD,  $93 \pm 91$  mo; range, 4–300 mo) after primary therapy were prospectively imaged with 4 techniques:  $^{18}\text{F}$ -DOPA PET/CT,  $^{18}\text{F}$ -FDG PET/CT, MDCT, and MRI. Images were analyzed for pathologic lesions, which were surgically removed when possible. The correlation between the detection rate for each method and the calcitonin and CEA concentrations and histopathologic findings was investigated. **Results:** On the basis of histology and follow-up, one or more imaging methods accurately localized metastatic disease in 12 (63%) of 19 patients. The corresponding figures for  $^{18}\text{F}$ -DOPA PET/CT,  $^{18}\text{F}$ -FDG PET/CT, MDCT, and MRI were 11 (58%) of 19, 10 (53%) of 19, 9 (47%) of 19, and 10 (59%) of 17, respectively. Calcitonin and CEA correlated with  $^{18}\text{F}$ -DOPA PET/CT ( $P = 0.0007$  and  $P = 0.0263$ , respectively) and  $^{18}\text{F}$ -FDG PET/CT findings (both  $P < 0.0001$ ). In patients with an unstable calcitonin doubling time ( $n = 8$ ),  $^{18}\text{F}$ -DOPA and  $^{18}\text{F}$ -FDG PET/CT were equally sensitive. In contrast, for patients with an unstable CEA doubling time ( $n = 4$ ),  $^{18}\text{F}$ -FDG PET/CT was more accurate. **Conclusion:** For most MTC patients with occult disease,  $^{18}\text{F}$ -DOPA PET/CT accurately detects metastases. In patients with an unstable calcitonin level,  $^{18}\text{F}$ -DOPA PET/CT and  $^{18}\text{F}$ -FDG PET/CT are complementary. For patients with an unstable CEA doubling time,  $^{18}\text{F}$ -FDG PET/CT may be more feasible. MRI is sensitive but has the highest rate of false-positive results.

**Key Words:** 18-fluorodeoxyglucose; 18-fluorodehydroxyphenylalanine; medullary thyroid cancer

**J Nucl Med 2011; 52:1855–1863**

DOI: 10.2967/jnumed.111.094771

**M**edullary thyroid cancer (MTC) is a rare malignancy arising from the parafollicular thyroid C cells (1). Surgery is the only possible curative therapy. Prognostic factors include postoperative tumor burden and serum calcitonin concentration (2). Recently, promising results with systemic therapy including multikinase inhibitors (3) and pre-targeted radioimmunotherapy have been reported (4). The primary treatment is total thyroidectomy, often including modified neck lymph node dissection. Follow-up is based on the tumor markers calcitonin and carcinoembryonic antigen (CEA) and neck ultrasonography (5). Persistent or increasing serum calcitonin and CEA levels imply residual or recurrent disease, but conventional imaging frequently remains negative. Calcitonin is the most sensitive marker and typically increases long before neck ultrasonography or CT demonstrates pathologic lymph nodes or distant metastases (6). Early and precise localization of residual or recurrent disease plays a mainstay role in planning the subsequent therapy. This would include surgery of locoregional metastatic disease or, for patients with distant metastatic spread, one of the new systemic treatment modalities and possibly palliative debulking surgery.

Diagnostic imaging of recurrent or residual MTC is difficult, and current conventional imaging techniques lack sensitivity. However, there have been encouraging results with PET using various tracers, and integrated PET/CT has improved the diagnostic accuracy.  $^{18}\text{F}$ -FDG is widely used

---

Received Jun. 22, 2011; revision accepted Sep. 12, 2011.  
For correspondence or reprints contact: Saila Kauhanen, Turku PET Centre, Turku University Hospital, P.O. Box 52, FIN-20521, Turku, Finland.  
E-mail: saila.kauhanen@utu.fi  
<sup>\*</sup>Contributed equally to this work.  
Published online Nov. 3, 2011.  
COPYRIGHT © 2011 by the Society of Nuclear Medicine, Inc.

in oncologic imaging; dihydroxyphenylalanine ( $^{18}\text{F}$ -DOPA) PET represents a new imaging tool in MTC (7–10).

The aim of the present study was to evaluate which imaging technique is best suited for the detection of metastatic MTC and whether the suitability is influenced by calcitonin and CEA concentrations. We prospectively compared the results of conventional imaging methods (multidetector CT [MDCT] and MRI) with those of PET/CT using  $^{18}\text{F}$ -FDG and  $^{18}\text{F}$ -DOPA in a series of MTC patients with recurrent or persistent disease, as evidenced by increased calcitonin or CEA concentrations on follow-up. The lesions detected were surgically removed when possible. To rule out false-positive imaging results, imaging results were compared with histologic results. Furthermore, we compared the tumor proliferation marker Ki-67 index (%) of all primary tumors with that of the metastases removed. The effect of surgery on marker concentrations was also evaluated.

## MATERIALS AND METHODS

### Patients and Study Design

This was a prospective, controlled multicenter trial including patients with residual or recurrent MTC after primary surgery. Between August 2007 and October 2009, 19 consecutive patients (10 men and 9 women; age range, 31–74 y; mean age, 51.6 y) with histologically proven MTC and increased calcitonin or CEA tumor markers were prospectively imaged using  $^{18}\text{F}$ -DOPA PET/CT,  $^{18}\text{F}$ -FDG PET/CT, MDCT, and MRI. All patients had undergone total thyroidectomy as the initial therapy. Patient characteristics are given in Supplemental Table 1 (supplemental materials are available online only at <http://jnm.snmjournals.org>). Patients 4, 8, and 17 had familial MTC (multiple endocrine neoplasia, type 2). Two patients could not undergo MRI because of a metallic foreign body or claustrophobia. All imaging methods were conducted within 6 wk. Twelve patients underwent surgery or had histopathologic confirmation of disease, 6 patients were followed up (range, 9–37 mo after imaging studies; mean  $\pm$  SD,  $15.7 \pm 10.9$  mo), and 1 patient died after 3 mo of follow-up because of progressive aggressive MTC; autopsy was not done. The study was conducted according to the guidelines of the Declaration of Helsinki, and the study protocol was approved by the ethics committee of the Hospital District of Southwest Finland. All patients gave written informed consent before participating in the study.

### $^{18}\text{F}$ -FDG PET/CT Protocol

$^{18}\text{F}$ -FDG PET/CT was done using a Discovery PET/CT STE scanner (GE Healthcare) at Turku PET Centre ( $n = 10$ ) or a Gemini GXL PET/CT scanner (Philips) at Helsinki PET Centre ( $n = 9$ ). The patients fasted for 6 h before the study. The dose of intravenous  $^{18}\text{F}$ -FDG was  $377 \pm 30$  MBq. Approximately 60 min after injection, a static  $^{18}\text{F}$ -FDG PET/CT scan in 3 dimensions covering the upper torso from eyebrows to mid thighs (3-min emission scan per position) started. Attenuation correction was performed using a low-dose ultrafast CT protocol (80 mAs, 140 kV, 0.3 mSv per field of view). Transaxial, coronal, and sagittal images for visual and semiquantitative analysis of the data were corrected for dead time, decay, and photon attenuation and reconstructed in a  $128 \times 128$  matrix. Images were reconstructed using 2 iterations and 28 subsets with a postprocessing filter of 6.0 mm in full width at half maximum and fully 3-dimensional maximum-

likelihood ordered-subset expectation maximization. Any focal tracer accumulation exceeding normal regional tracer uptake was considered pathologic. PET images were analyzed visually and semiquantitatively by calculating mean and maximum standardized uptake value ( $\text{SUV}_{\text{max}}$ ), defined as the ratio of activity per milliliter of tissue to the activity in the injected dose corrected by decay and by the patient's body weight. A 1-cm-diameter ( $0.77 \text{ cm}^3$ ) region of interest was placed on the area of the lesion with the highest uptake.

### $^{18}\text{F}$ -DOPA PET/CT Protocol

All  $^{18}\text{F}$ -DOPA PET/CT studies were performed at Turku PET Centre. The patients fasted for at least 6 h before undergoing PET/CT. If the patient was taking medication that could affect the biodistribution of  $^{18}\text{F}$ -DOPA (diazoxide or cortisone), this medication was withdrawn 24 h before the study. All  $^{18}\text{F}$ -DOPA PET/CT scans were acquired using the Discovery PET/CT STE scanner.  $^{18}\text{F}$ -DOPA was synthesized as previously described (11). The average administered dose of  $^{18}\text{F}$ -DOPA was  $243 \pm 46$  MBq. The decarboxylase inhibitor, carbidopa, was given as premedication. Scanning began approximately 60 min after tracer injection. Patients underwent a whole combined PET/CT scan from the level of the eyes to the mid thigh. This CT-based scan was used for attenuation correction and to help in anatomic localization of  $^{18}\text{F}$ -DOPA uptake. Immediately after the CT, an emission PET scan was acquired in the 3-dimensional mode over the same anatomic regions, starting at the level of the mid thigh. To obtain images for visual and semiquantitative analysis, we corrected the data for dead time, decay, and photon attenuation and reconstructed the data in a  $128 \times 128$  matrix. The images were reconstructed and analyzed as described for the  $^{18}\text{F}$ -FDG PET/CT protocol.

### MDCT Protocol

MDCT images were acquired at 5 centers using 7 different CT scanners. The number of detector rows for the scanners ranged from 6 to 64. The final reconstructed axial slice thickness ranged from 2.5 to 6.5 mm. All patients received iodinated contrast medium. In 5 patients, an unenhanced study of the upper abdomen was performed first, followed by contrast administration and imaging in the arterial and venous phases. Seven patients were imaged after contrast administration only in the arterial and venous phases, and 2 patients were imaged in arterial, venous, and 5-min delayed phases. Five patients were imaged in the venous phase only.

### MRI Protocol

MRI of the neck and thorax was performed using a 1.5-T system (Gyrosan Intera Nova Dual; Philips Medical Systems) with a head-neck coil. First, T1-weighted transaxial and coronal turbo spin-echo images were obtained. In addition, we acquired T1-weighted spectral fat-saturated inversion recovery transaxial images. After injection of gadolinium ( $0.2 \text{ mL/kg}$  of patient weight; Dotarem [Guerbet]), spectral fat-saturated inversion recovery T1-weighted turbo spin-echo images were acquired in all (transaxial, sagittal, and coronal) dimensions. A 25-cm field of view was used. The slice thickness was 4 mm in all acquisitions. Thereafter, 7-mm T1- and T2-weighted transaxial turbo spin-echo images of the mediastinum and thorax were obtained.

### Data Evaluation

$^{18}\text{F}$ -DOPA- and  $^{18}\text{F}$ -FDG-avid lesions were recorded per patient and per region in 5 distinct regions: neck, mediastinum,

lungs, liver, and skeleton. Lymph nodes larger than 10 mm in the smallest diameter were diagnosed as malignant on MRI and MDCT. In addition, the tissues taken during primary surgery and during reoperations were prepared for immunohistochemical examination (cell cycle-associated Ki-67 antigen) and were reanalyzed by an experienced pathologist.

The diagnostic accuracy of the imaging studies was assessed by comparison of histopathologic reports on lesions removed ( $n = 12$ ) with imaging findings. When histologic reports were not available, a consensus based on the sum of the imaging procedures and data from follow-up examinations was reached ( $n = 7$ ). Lesion site and axis were taken from pathologic reports if the patient had undergone surgery; otherwise, lesion site and axis were taken from imaging studies. All regions and lesions seen on different imaging modalities were calculated. If more than 10 lesions were present, the number of lesions was truncated at 10 to avoid bias toward that region. Each type of imaging study ( $^{18}\text{F}$ -DOPA PET/CT,  $^{18}\text{F}$ -FDG PET/CT, MDCT, and MRI) was interpreted in a masked manner by a different observer.

### Statistical Analysis

The results are expressed mainly as mean values  $\pm$  SD of the mean. The sensitivity of  $^{18}\text{F}$ -FDG PET/CT,  $^{18}\text{F}$ -DOPA PET/CT, MDCT, and MRI for lesion detection was calculated using the pathologic results and clinical follow-up as a gold standard, with a  $2 \times 2$  contingency table. A McNemar test was performed to compare  $^{18}\text{F}$ -FDG PET/CT,  $^{18}\text{F}$ -DOPA PET/CT, MDCT, and MRI results. The  $\kappa$ -coefficient was determined to quantify agreement between these imaging methods and calcitonin and CEA doubling time. Doubling times were determined according to the calculator provided by the American Thyroid Association (<http://www.thyroid.org/professionals/calculators/CDTC.php>). The Wilcoxon signed-rank test was used to evaluate the number of regions and lesions diagnosed. For the receiver operating characteristics, analysis of sensitivities for different cutoff points of calcitonin and CEA were calculated. A  $P$  value of less than 0.05 was considered statistically significant. All statistical analyses were performed with SAS software (version 9.2; SAS Institute Inc.).

## RESULTS

### Relation of Histologic Data and Clinical Follow-up to Imaging Findings

All study patients had biochemically proven residual or recurrent disease and were therefore suspected of having metastases. Fifteen patients showed pathologic findings on study imaging, 11 of whom subsequently underwent surgery. Eight of these patients were histologically confirmed to have metastatic MTC, and 3 had a benign histologic type (Fig. 1, Table 1). In addition, 1 patient (patient 17) had disseminated disease and underwent surgery because of pheochromocytoma, but no histologic data were available from the metastases. In 3 of 15 imaging-positive patients, no histologic data were available, but disseminated disease was obvious on imaging (Fig. 1). Two of these patients (patients 9 and 10) died after 9 and 3 mo, respectively, of follow-up, and autopsies were not performed. One patient (patient 14) received symptomatic treatment because surgery was considered impossible. In the remaining 4 patients (patients 1, 12, 15, and 16), all 4 imaging techniques were negative. Also

these patients were suspected of having residual disease because of an increased calcitonin level (range, 13.8–69.4 pmol/L; normal,  $<1.7$  pmol/L [women] and  $<3.8$  pmol/L [men]), an increased CEA level (range, 2.0–7.3  $\mu\text{g/L}$ ; normal,  $<3.5$   $\mu\text{g/L}$ ), or both. In one of these patients (patient 1), metastatic MTC was confirmed on follow-up 37 mo later with MDCT.

**Patient-by-Patient Analysis.** In patient-based analysis, metastatic lesions were shown in 11 of 19 patients on  $^{18}\text{F}$ -DOPA PET/CT and in 10 of 19 patients on  $^{18}\text{F}$ -FDG PET/CT. Normal imaging results in these patients were classified as false-negative. The diagnostic per-patient detection rates were 58% (95% confidence interval [CI], 35.7%–80.1%) for  $^{18}\text{F}$ -DOPA PET/CT, 53% (95% CI, 30.2%–75.1%) for  $^{18}\text{F}$ -FDG PET/CT, 47% (95% CI, 30.2%–75.1%) for MDCT, and 59% (95% CI, 35.4%–82.2%) for MRI. Because of the small sample size, the McNemar test did not show any method to have any significant additional value for diagnosis of metastatic MTC. The detection rate of multimodality imaging was 74% (95% CI, 53.9%–93.5%) for both  $^{18}\text{F}$ -DOPA and  $^{18}\text{F}$ -FDG PET/CT and 68% (95% CI, 47.5%–89.3%) for conventional imaging (MDCT and MRI) ( $P = 0.5637$ ).

**Region-by-Region and Lesion-by-Lesion Analysis.** The total number of lesions detected in 5 regions (neck, lungs, mediastinum, liver, and bone) is shown in Supplemental Table 2.

In region-based analysis, 26 (27%) of 95 regions evaluated were considered metastatic on the basis of the reference standard (histology [ $n = 11$ ] or a lesion demonstrated by at least 2 imaging methods [ $n = 12$ ]). In 4 regions, only 1 method revealed a metastasis: patients 6 and 19 had lesions in the mediastinum on MRI, patient 9 had lesions in the neck on  $^{18}\text{F}$ -DOPA PET/CT, and patient 18 had a lesion in the lungs on MRI. In these patients, metastases had been detected also in other regions.

In lesion-based analysis, 118 lesions were considered metastatic on the basis of the reference standard.  $^{18}\text{F}$ -DOPA PET/CT detected 61 (52%) of 118 lesions;  $^{18}\text{F}$ -FDG PET/CT, 55 lesions (47%); MDCT, 54 lesions (46%); and MRI, 92 lesions (78%). Compared with other imaging methods, MRI detected most lesions for each region analyzed (neck, lung, liver, and bone) except for the mediastinum (16 by MRI vs. 24 by  $^{18}\text{F}$ -DOPA PET/CT). On the basis of the

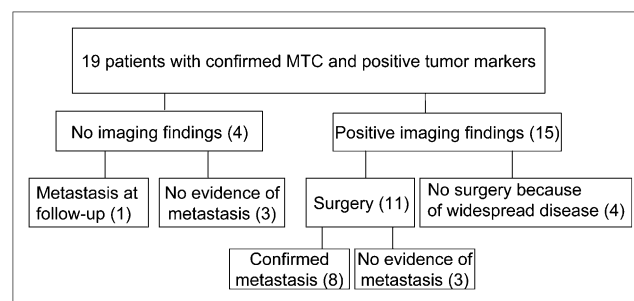


FIGURE 1. Patient flow chart.

**TABLE 1**  
Comparison of Different Imaging Methods, Calcitonin and CEA Doubling Time, and Ki-67 Expression

Patient no.	Ki-67 (%) in primary operation (primary tumor/metastasis)	Number of lesions				Doubling time (mo)		Ki-67(%) in recurrence	Histologic verification or follow-up
		<sup>18</sup> F-DOPA PET/CT	<sup>18</sup> F-FDG PET/CT	MDCT	MRI	Calcitonin	CEA		
1	1	0	0	0	0	8.3	61.7	5*	F-U: 37 mo†
2	10	1	1	1	1	4.3	9.3	15	H: metastasis in neck (20 mm)
3	1	1	1	0	0	31.4	51.0	2	H: metastasis (6 mm)
4	5	4‡	4‡	2‡	>10‡	24.3	171.0	5	H: resection of rib, neck dissection, biopsy of liver
5	2	0	2 FP	2 FP	1 FP	76.0	122.0	—	H: benign neck lymph node
6	2	6	2 (+1 FP)	2	5	42.0	28.7	30	H: metastasis (10 mm)
7	2	1	1	1	1	28.3	67.0	5	H: metastasis (19 mm)
8	1	1	0	0	3 FP	28.3	NA	—	H: parathyroid adenoma and benign neck lymph node
9	2	>10	1	>10	>10	16.0	NA	—	F-U: exitus, no H
10	30/30	0	>10	>10	>10	10.8	13.7	—	F-U: exitus, no H
11	2	1	0	0	0	54.9	122.0	5	H: metastasis
12	5	0	0	0	0	239.5	190.0	—	F-U: 17 mo
13	5	0	0	0	1 FP	8.2	8.5	—	H: benign neck lymph node
14	20/5	10	8	8	8	14.7	84.0	—	F-U: no H, 11 mo
15	2/2	0	0	0	ND§	27.4	98.5	—	F-U: 11 mo
16	2	0	0	0	ND	154.4	180.0	—	F-U: 9 mo
17	2	5¶	10¶	7	8	25.1	40.8	—	F-U: H only from pheochromocytoma
18	60/60	>10	10	7	>10	0.35	2.10	60	H: metastasis (30 mm)
19	5	3	0	0	7	19.5	NA	5	H: metastasis (7 mm)

\*Metastatic lesion in neck detected after 37 mo of follow-up.

†Neck metastasis detected at end of follow-up (37 mo) and operated on.

‡Lesions were detected in different regions.

§Due to claustrophobia.

||Due to metallic foreign body.

¶Both <sup>18</sup>F-DOPA and <sup>18</sup>F-FDG PET/CT showed pheochromocytoma.

F-U = follow-up; H = histologic verification; FP = false-positive; NA = not applicable; ND = not determined.

reference standard, a total of 7 lesions were considered false-positive: 6 on MRI, 2 on <sup>18</sup>F-FDG PET/CT, and 1 each on <sup>18</sup>F-DOPA PET/CT and MDCT. The mean SUV<sub>max</sub> of all lesions was 3.57 ± 4.59 for <sup>18</sup>F-DOPA PET/CT and 2.55 ± 2.87 for <sup>18</sup>F-FDG PET/CT.

#### Tumor Markers and Histopathology and Correlation with Imaging Findings

**Calcitonin and CEA.** Calcitonin and CEA concentrations at the time of imaging are given in Supplemental Table 1. Calcitonin was higher in patients with positive imaging findings and was only marginally increased in those with false-negative findings (Wilcoxon correlation coefficient,  $P = 0.0015$ ). The best discriminative value for detecting metastasis with any of the imaging methods was a cutoff of 54.0 pmol/L (normal value, <3.8 pmol/L for men and <1.7

pmol/L for women) for calcitonin in receiver-operating characteristic analysis. When calculated for each different imaging method separately, the cutoff was 44.8 pmol/L for <sup>18</sup>F-DOPA PET/CT, 56.8 pmol/L for <sup>18</sup>F-FDG PET/CT, 72.0 pmol/L for MDCT, and 62.9 pmol/L for MRI. Both calcitonin and CEA correlated with the number of lesions diagnosed on <sup>18</sup>F-DOPA PET/CT ( $P = 0.0007$  and  $0.0263$ , respectively, Fig. 2A). Lesions detected with <sup>18</sup>F-FDG PET/CT correlated strongly with both calcitonin and CEA ( $P < 0.0001$ ) (Fig. 2B). This correlation was observed also with MDCT and MRI. In addition, calcitonin and CEA correlated significantly with <sup>18</sup>F-FDG PET/CT SUV<sub>max</sub> (the highest SUV<sub>max</sub> of all lesions was considered) ( $P < 0.0001$  and  $P = 0.0006$ , respectively). The same trend was observed between calcitonin ( $P = 0.0158$ ) or CEA ( $P = 0.0553$ ) level and SUV<sub>max</sub> of <sup>18</sup>F-DOPA PET/CT.

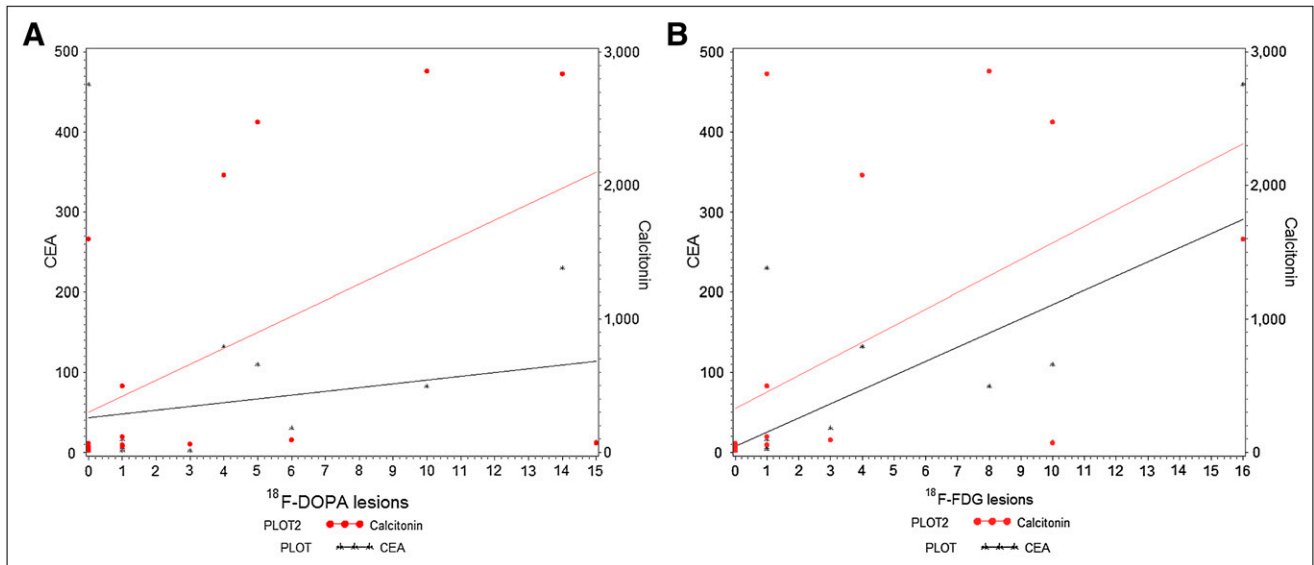


**FIGURE 2.** (A) Calcitonin and CEA correlation for number of lesions detected on  $^{18}\text{F}$ -DOPA PET/CT. (B) Calcitonin and CEA correlation for number of lesions detected on  $^{18}\text{F}$ -FDG PET/CT.

Tumor markers decreased postoperatively in 4 of 8 operated patients with histologic verification of metastasis (patients 2, 3, 7, and 11). In these patients, only 1 metastasis was detected and then radically operated on. In 3 patients (patients 6, 18, and 19), tumor markers remained unchanged; of these, patients 6 and 18 underwent debulking surgery. In 1 patient (patient 4), tumor markers continued to increase after debulking surgery (Table 1).

*Calcitonin and CEA Doubling Time.* Tumor marker doubling time (mo) and imaging results are presented in Table 1. Calcitonin and CEA doubling time was inversely related to the number of lesions diagnosed on  $^{18}\text{F}$ -FDG PET/CT; these correlations were borderline-significant

( $P = 0.0798$  and  $0.0546$ , respectively) (Fig. 3A). Calcitonin and CEA doubling time (mo) did not correlate with the number of lesions detected on  $^{18}\text{F}$ -DOPA PET/CT ( $P = 0.2142$  and  $0.2393$ , respectively) (Fig. 3B). Eighty percent of patients with a calcitonin doubling time of less than 24 mo (denoting unstable disease,  $n = 8$ ) had a positive finding on at least 1 imaging technique; the corresponding figure for patients with a calcitonin doubling time of more than 24 mo (denoting stable disease,  $n = 11$ ) was 44%. The  $\kappa$ -coefficient for agreement was positive for unstable or stable calcitonin level and CEA doubling time and detection or no detection of recurrent disease ( $\kappa = 0.36$  and  $0.28$ , respectively). The total number of lesions detected using

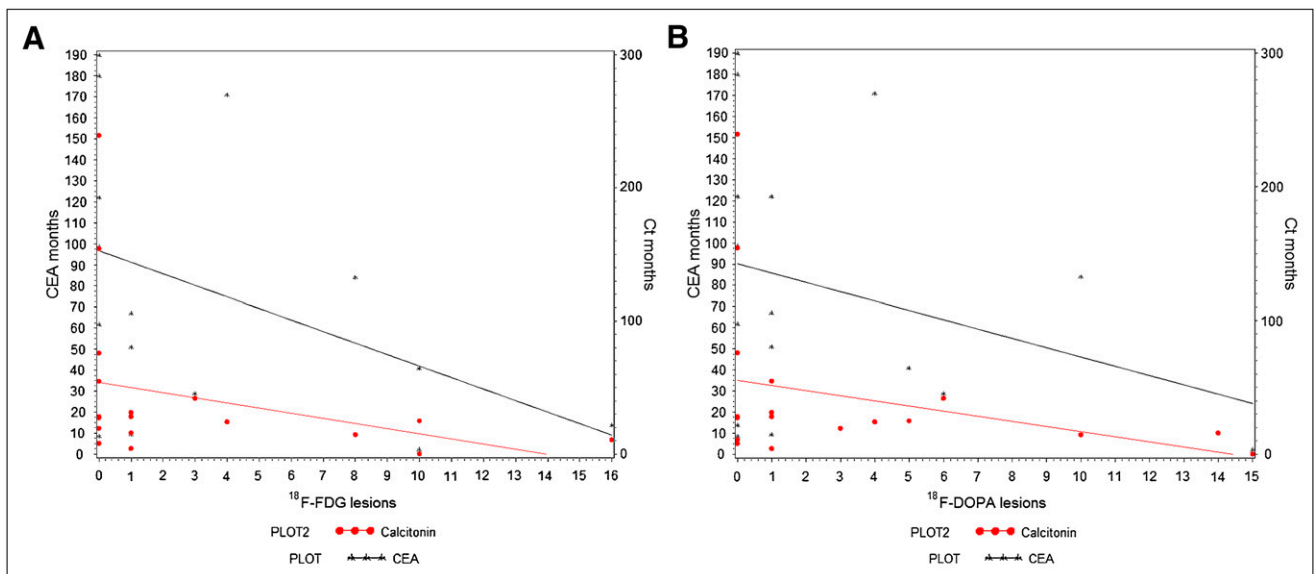


**FIGURE 3.** (A) CEA and calcitonin doubling time (mo) for number of lesions detected on  $^{18}\text{F}$ -FDG PET/CT. (B) CEA and calcitonin doubling time (mo) for number of lesions detected on  $^{18}\text{F}$ -DOPA PET/CT. Ct = calcitonin.

the different imaging methods is shown in Figure 4. For a calcitonin doubling time of less than 24 mo, metastases were detected in 70% of patients with both  $^{18}\text{F}$ -DOPA and  $^{18}\text{F}$ -FDG PET/CT. In contrast, for a CEA doubling time of less than 24 mo,  $^{18}\text{F}$ -FDG PET/CT correctly detected metastases in 80% of patients and  $^{18}\text{F}$ -DOPA PET/CT in 60%.

**Histopathology.** Histopathologic data were reanalyzed by an experienced pathologist without knowledge of imaging findings. The Ki-67 proliferation index was determined for all primary tumors and for lesions removed that proved to be metastases ( $n = 9$ ) (Table 1). In 6 of 9 patients, Ki-67 was higher in the metastases than in the primary tumor. Two patients with primary tumor proliferation indices of 30% and 60% (patients 10 and 18, Table 1) had aggressive disease and died a few months after diagnosis.

Figure 5 demonstrates a patient (patient 11) with a calcitonin level of 44.8 pmol/L in whom a neck metastasis with a low proliferation index of 5% was detected on  $^{18}\text{F}$ -DOPA PET/CT, whereas  $^{18}\text{F}$ -FDG PET/CT, MDCT, and MRI remained negative. Figure 6 demonstrates a patient with aggressive disease.

## DISCUSSION

To our knowledge, this was the first prospective study comparing combined  $^{18}\text{F}$ -DOPA and  $^{18}\text{F}$ -FDG PET/CT

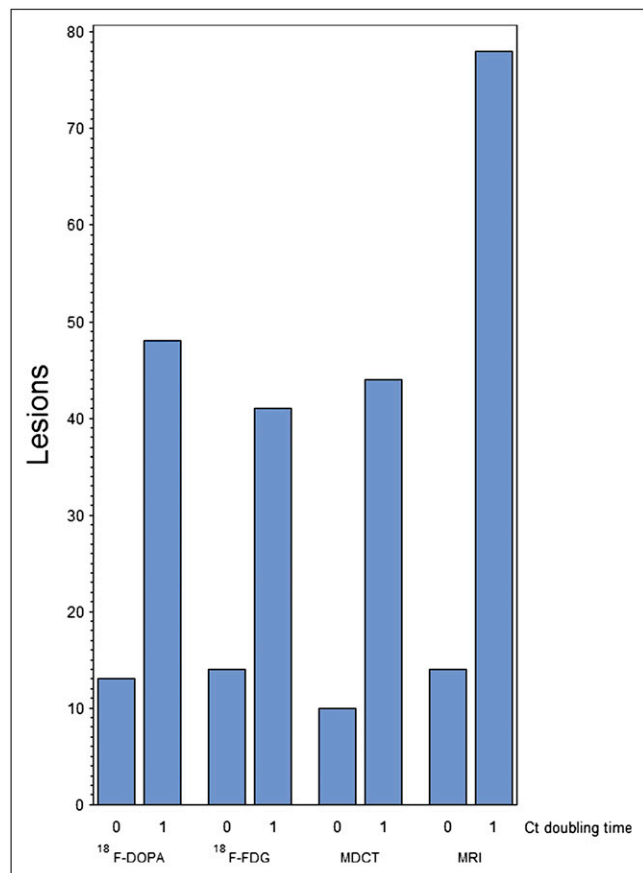


**FIGURE 4.** Total number of lesions detected using different imaging techniques in stable (0) and unstable (1) tumor marker groups. Ct = calcitonin.

with conventional MDCT and MRI in MTC patients with increased calcitonin and CEA concentrations. The detected lesions were surgically removed when possible and examined histopathologically. Our study showed that metastatic disease was accurately localized in 12 (63%) of 19 patients on combined imaging, in 11 (56%) of 19 on  $^{18}\text{F}$ -DOPA PET/CT, in 10 (53%) of 19 on  $^{18}\text{F}$ -FDG PET/CT, and in 9 (47%) of 19 on MDCT. MRI was performed on 17 patients and detected most lesions but had the highest rate of false-positive results. Importantly, in a patient with a calcitonin level of only 44.8 pmol/L,  $^{18}\text{F}$ -DOPA PET/CT was the only imaging method that accurately localized a metastasis with a Ki-67 of 5% in the neck.  $^{18}\text{F}$ -DOPA PET/CT may be of particular value for detection of occult metastatic MTC characterized by a low proliferation index. In MTC patients with increasing calcitonin levels during follow-up,  $^{18}\text{F}$ -DOPA PET/CT and  $^{18}\text{F}$ -FDG PET/CT have complementary roles. Although the number of patients with an unstable CEA doubling time ( $<24$  mo) was small ( $n = 4$ ), our data support the notion that imaging with  $^{18}\text{F}$ -FDG PET/CT rather than  $^{18}\text{F}$ -DOPA PET/CT is better for such patients, as indicated by the higher detection rate for metastatic disease. Bogsrud et al. (12) evaluated the prognostic value of  $^{18}\text{F}$ -FDG PET and found that calcitonin doubling time was shorter for PET-positive than -negative patients. Our finding is in concordance with that study. It is clear that the results are affected by the subtypes of MTC included in the different studies, which may vary from occult disease that remains stable over 10–20 y to aggressive disease that shortens the life span.

Several studies have shown that  $^{18}\text{F}$ -FDG PET has better sensitivity than conventional imaging in MTC (13–18). In line with the present study,  $^{18}\text{F}$ -FDG uptake in MTC correlates with poor differentiation and limited tracer uptake (19,20). There is therefore a need for PET tracers other than  $^{18}\text{F}$ -FDG. MTC comprises neuroendocrine tumors capable of taking up and decarboxylating amine precursors. As demonstrated by Ahlström et al. in 1995 with  $^{11}\text{C}$ -labeled DOPA (21),  $^{18}\text{F}$ -DOPA has been used in the diagnosis of carcinoids (22–24), pheochromocytomas (25,26), glomus tumors (27), and pancreatic neuroendocrine tumors (28). Only a few studies have evaluated the value of  $^{18}\text{F}$ -DOPA PET in MTC (7,8,29) and even fewer have used integrated  $^{18}\text{F}$ -DOPA-PET/CT (9,30,31).

A preliminary study on  $^{18}\text{F}$ -DOPA PET in MTC reported a total of 27 tumors in 11 patients using  $^{18}\text{F}$ -DOPA PET (7). The sensitivity was 63% for  $^{18}\text{F}$ -DOPA PET, 44% for  $^{18}\text{F}$ -FDG, 52% for SRS, and 81% for morphologic imaging. Although morphologic imaging procedures had the best sensitivity, the specificity for primary tumors or local recurrence and lymph node metastases was low (55%–57%). Our study confirmed these results: MRI had the highest detection rate (78%) in lesion-based analysis, but 6 of 7 false-positive results were obtained by MRI. A retrospective study on combined  $^{18}\text{F}$ -DOPA PET/CT showed that  $^{18}\text{F}$ -DOPA PET/CT had the highest sensitivity (74%), com-

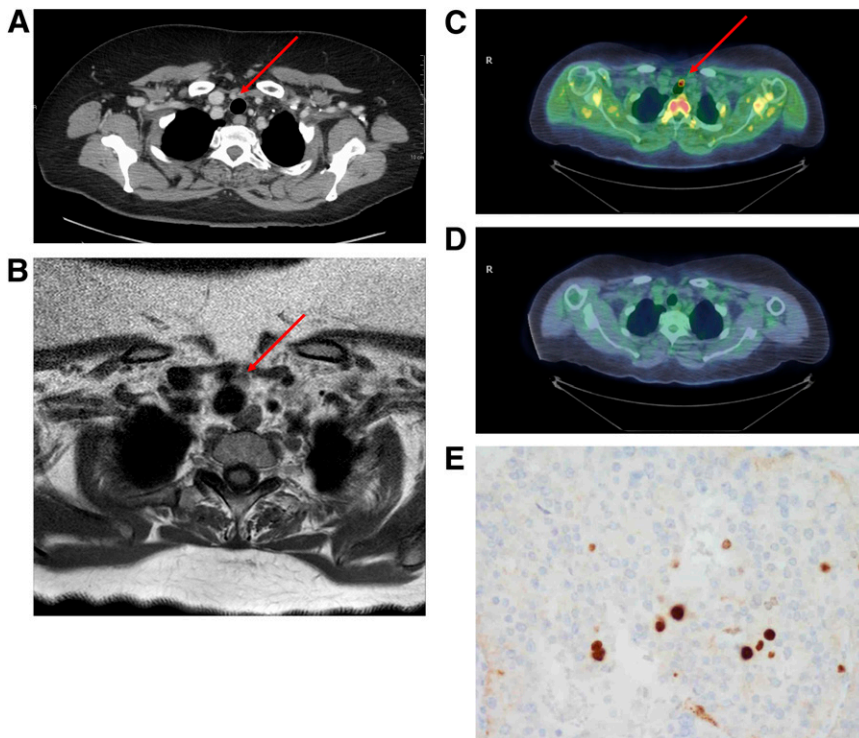


**FIGURE 5.** 61-y-old woman (patient 11) with occult MTC and calcitonin level of 44.8 pmol/L 9 y after primary therapy. Imaging with MDCT (A) and MRI (B) was negative.  $^{18}\text{F}$ -DOPA PET/CT (C) demonstrated increased uptake of  $^{18}\text{F}$ -DOPA in neck.  $^{18}\text{F}$ -FDG PET/CT (D) was negative. Lesion was surgically removed; histology was compatible with lymph node metastasis, and Ki-67 was 5% (E).

pared with other methods (i.e., PET alone [52%] or CT [68%]) (9).

Approximately 40% of MTC patients have persistent disease as indicated by increased calcitonin concentrations after primary surgery, and 10% with undetectable post-operative calcitonin still have occult disease and develop recurrence later (1). We demonstrated a strong correlation between metastatic lesions and calcitonin concentration, with a calcitonin cutoff of 157 pg/mL (44.8 pmol/L) for  $^{18}\text{F}$ -DOPA PET/CT in receiver-operating-characteristic analysis. Furthermore,  $^{18}\text{F}$ -DOPA PET/CT was able to detect lesions at lower calcitonin concentrations than the other methods, in line with Luster et al. (9), who reported a sensitivity of 100% for a calcitonin level higher than 150 pg/mL. These findings differ from Koopmans et al. (8), who found 75% negative scans in patients with calcitonin concentrations of less than 500 pg/mL, and from that of Hoergerle et al. (7), who found no MTC-positive  $^{18}\text{F}$ -DOPA PET scans if the calcitonin level was less than 550 pg/mL. Further, Marzola et al. found higher calcitonin concentrations in PET-positive than -negative patients but did not notice any difference between the tracers used ( $^{18}\text{F}$ -FDG or  $^{18}\text{F}$ -DOPA) (31). The American Thyroid Association recently recommended additional imaging in MTC in patients with a postsurgical calcitonin level of 150 pg/mL or greater (32), and our results are in line with this result.

A strength of the present study was that it showed improvement of anatomic localization using combined PET/CT. To the best of our knowledge, this was the first study in which PET/CT using 2 different tracers was compared with both dedicated MDCT and MRI. Further-

more, we used carbidopa medication before  $^{18}\text{F}$ -DOPA PET/CT. Several groups have suggested that inhibiting the peripheral decarboxylation enhances tumor accumulation of DOPA and 5-hydroxy-L-tryptophan (26,33,34). In previous studies on MTC and  $^{18}\text{F}$ -DOPA PET, only the groups of Beuthien-Baumann and Koopmans (8,29) used carbidopa premedica-

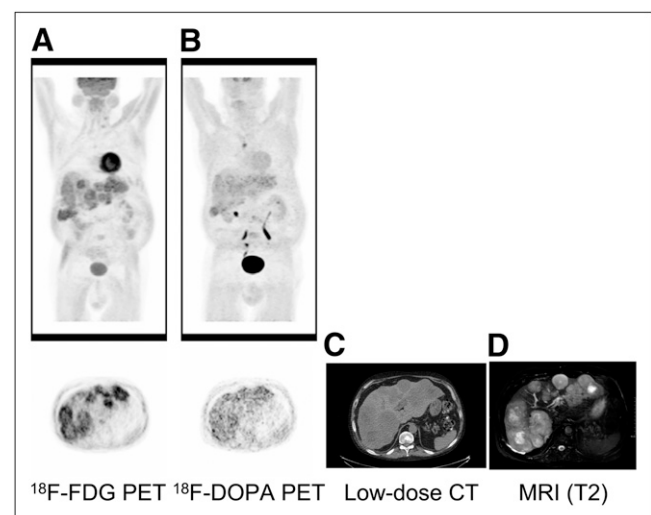


**FIGURE 6.** 56-y-old man (patient 10) with aggressive MTC and high primary tumor Ki-67 of 30%. Two years after primary treatment, calcitonin level was 1,598 pmol/L and CEA 460  $\mu\text{g/L}$ , with unstable calcitonin and CEA doubling time (10 mo).  $^{18}\text{F}$ -FDG PET/CT demonstrated disseminated disease (A, several lesions in liver, skeleton, neck, and paraaortic region), but  $^{18}\text{F}$ -DOPA PET/CT was negative (B). MDCT (C) and MRI (D) showed lesions in liver, skeleton, and neck. Patient died 3 mo after imaging.

tion. Furthermore, we assumed that all study patients had at least microscopic disease as evidenced by increased tumor marker concentrations, and we concluded that none of the patients should have true negative imaging.

The major limitation of the present study was the relatively small number of patients, as the disease is rare. Although sample size limits the analysis, our study was unique because it included a population imaged prospectively with 4 different methods. However, the MDCT protocol was not performed on all patients and varied between different institutions.

## CONCLUSION

To the best of our knowledge, no previous studies have prospectively compared  $^{18}\text{F}$ -DOPA and  $^{18}\text{F}$ -FDG PET/CT with both MDCT and MRI. On the basis of our results,  $^{18}\text{F}$ -DOPA and  $^{18}\text{F}$ -FDG PET/CT are useful complementary imaging tools for accurate identification of metastases both in MTC patients with occult disease and in MTC patients with more aggressive disease. Accurate detection of metastatic disease is a prerequisite for tailoring further treatment, that is, surgery, pretargeted radioimmunotherapy, or multikinase inhibitor treatment.

## DISCLOSURE STATEMENT

The costs of publication of this article were defrayed in part by the payment of page charges. Therefore, and solely to indicate this fact, this article is hereby marked "advertisement" in accordance with 18 USC section 1734.

## ACKNOWLEDGMENTS

We thank the staffs of the Turku and Helsinki PET Centres, the Turku Cyclotron, and the Radiochemistry Laboratory. We also thank Marketta Halinen. This study was supported by grants from Research Funding of Helsinki and Turku University Central Hospital (Eryitysvaltionosuus) and the Cancer Foundation of South-West Finland. No other potential conflict of interest relevant to this article was reported.

## REFERENCES

1. Kebebew E, Ituarte PH, Siperstein AE, Duh QY, Clark OH. Medullary thyroid carcinoma: clinical characteristics, treatment, prognostic factors, and a comparison of staging systems. *Cancer*. 2000;88:1139–1148.
2. Schröder S, Bocker W, Baisch H, et al. Prognostic factors in medullary thyroid carcinomas: survival in relation to age, sex, stage, histology, immunocytochemistry, and DNA content. *Cancer*. 1988;61:806–816.
3. Lam ET, Ringel MD, Kloos RT, et al. Phase II clinical trial of sorafenib in metastatic medullary thyroid cancer. *J Clin Oncol*. 2010;28:2323–2330.
4. Kraeber-Bodéré F, Salauin PY, Oudoux A, Goldenberg DM, Chatal JF, Barbet J. Pretargeted radioimmunotherapy in rapidly progressing, metastatic, medullary thyroid cancer. *Cancer*. 2010;116:1118–1125.
5. Busnardo B, Girelli ME, Simioni N, Nacamulli D, Busetto E. Nonparallel patterns of calcitonin and carcinoembryonic antigen levels in the follow-up of medullary thyroid carcinoma. *Cancer*. 1984;53:278–285.
6. Engelbach M, Gorges R, Forst T, et al. Improved diagnostic methods in the follow-up of medullary thyroid carcinoma by highly specific calcitonin measurements. *J Clin Endocrinol Metab*. 2000;85:1890–1894.

7. Hoegerle S, Althoefer C, Ghanem N, Brink I, Moser E, Nitzsche E.  $^{18}\text{F}$ -DOPA positron emission tomography for tumour detection in patients with medullary thyroid carcinoma and elevated calcitonin levels. *Eur J Nucl Med*. 2001;28:64–71.
8. Koopmans KP, de Groot JW, Plukker JT, et al.  $^{18}\text{F}$ -dihydroxyphenylalanine PET in patients with biochemical evidence of medullary thyroid cancer: relation to tumor differentiation. *J Nucl Med*. 2008;49:524–531.
9. Luster M, Karges W, Zeich K, et al. Clinical value of 18-fluorine-fluorodihydroxyphenylalanine positron emission tomography/computed tomography in the follow-up of medullary thyroid carcinoma. *Thyroid*. 2010;20:527–533.
10. Kauhane S, Seppanen M, Ovaska J, et al. The clinical value of [ $^{18}\text{F}$ ]fluorodihydroxyphenylalanine positron emission tomography in primary diagnosis, staging, and restaging of neuroendocrine tumors. *Endocr Relat Cancer*. 2009;16:255–265.
11. Bergman J, Haaparanta M, Lehtikoinen P, Solin O. Electrophilic synthesis of 6( $^{18}\text{F}$ )fluoro-L-dopa starting from aqueous-( $^{18}\text{F}$ )fluoride. *J Labelled Comp Radiopharm*. 1994;35:476–477.
12. Bogsrud TV, Karantanis D, Nathan MA, et al. The prognostic value of 2-deoxy-2-[ $^{18}\text{F}$ ]fluoro-D-glucose positron emission tomography in patients with suspected residual or recurrent medullary thyroid carcinoma. *Mol Imaging Biol*. 2010;12:547–553.
13. Gasparoni P, Rubello D, Ferlin G. Potential role of fluorine-18-deoxyglucose (FDG) positron emission tomography (PET) in the staging of primitive and recurrent medullary thyroid carcinoma. *J Endocrinol Invest*. 1997;20:527–530.
14. Diehl M, Risse JH, Brandt-Mainz K, et al. Fluorine-18 fluorodeoxyglucose positron emission tomography in medullary thyroid cancer: results of a multicenter study. *Eur J Nucl Med*. 2001;28:1671–1676.
15. Musholt TJ, Musholt PB, Dehdashti F, Moley JF. Evaluation of fluorodeoxyglucose-positron emission tomographic scanning and its association with glucose transporter expression in medullary thyroid carcinoma and pheochromocytoma: a clinical and molecular study. *Surgery*. 1997;122:1049–1060.
16. Szakáll S Jr, Bajzik G, Repa I, et al. FDG PET scan of metastases in recurrent medullary carcinoma of the thyroid gland [in Hungarian]. *Orv Hetil*. 2002;143 (21 suppl 3):1280–1283.
17. Brandt-Mainz K, Muller SP, Gorges R, Saller B, Bockisch A. The value of fluorine-18 fluorodeoxyglucose PET in patients with medullary thyroid cancer. *Eur J Nucl Med*. 2000;27:490–496.
18. de Groot JW, Links TP, Jager PL, Kahraman T, Plukker JT. Impact of  $^{18}\text{F}$ -fluoro-2-deoxy-D-glucose positron emission tomography (FDG-PET) in patients with biochemical evidence of recurrent or residual medullary thyroid cancer. *Ann Surg Oncol*. 2004;11:786–794.
19. Adams S, Baum R, Rink T, Schumm-Drager PM, Usadel KH, Hor G. Limited value of fluorine-18 fluorodeoxyglucose positron emission tomography for the imaging of neuroendocrine tumours. *Eur J Nucl Med*. 1998;25:79–83.
20. Adams S, Baum RP, Hertel A, Schumm-Drager PM, Usadel KH, Hor G. Metabolic (PET) and receptor (SPET) imaging of well- and less well-differentiated tumours: comparison with the expression of the Ki-67 antigen. *Nucl Med Commun*. 1998;19:641–647.
21. Ahlström H, Eriksson B, Bergstrom M, Bjurling P, Langstrom B, Oberg K. Pancreatic neuroendocrine tumors: diagnosis with PET. *Radiology*. 1995;195:333–337.
22. Hoegerle S, Althoefer C, Ghanem N, et al. Whole-body  $^{18}\text{F}$  dopa PET for detection of gastrointestinal carcinoid tumors. *Radiology*. 2001;220:373–380.
23. Becherer A, Szabo M, Karanikas G, et al. Imaging of advanced neuroendocrine tumors with  $^{18}\text{F}$ -FDOPA PET. *J Nucl Med*. 2004;45:1161–1167.
24. Koopmans KP, Neels OC, Kema IP, et al. Improved staging of patients with carcinoid and islet cell tumors with  $^{18}\text{F}$ -dihydroxy-phenyl-alanine and  $^{11}\text{C}$ -5-hydroxy-tryptophan positron emission tomography. *J Clin Oncol*. 2008;26:1489–1495.
25. Hoegerle S, Nitzsche E, Althoefer C, et al. Pheochromocytomas: detection with  $^{18}\text{F}$  DOPA whole body PET—initial results. *Radiology*. 2002;222:507–512.
26. Timmers HJ, Hadi M, Carrasquillo JA, et al. The effects of carbidopa on uptake of 6- $^{18}\text{F}$ -fluoro-L-DOPA in PET of pheochromocytoma and extraadrenal abdominal paraganglioma. *J Nucl Med*. 2007;48:1599–1606.
27. Hoegerle S, Ghanem N, Althoefer C, et al.  $^{18}\text{F}$ -DOPA positron emission tomography for the detection of glomus tumours. *Eur J Nucl Med Mol Imaging*. 2003;30:689–694.
28. Kauhane S, Seppanen M, Minn H, et al. Fluorine-18-L-dihydroxyphenylalanine ( $^{18}\text{F}$ -DOPA) positron emission tomography as a tool to localize an insulinoma or  $\beta$ -cell hyperplasia in adult patients. *J Clin Endocrinol Metab*. 2007;92:1237–1244.
29. Beuthien-Baumann B, Strumpf A, Zessin J, Bredow J, Kotzerke J. Diagnostic impact of PET with  $^{18}\text{F}$ -FDG,  $^{18}\text{F}$ -DOPA and 3-O-methyl-6-[ $^{18}\text{F}$ ]fluoro-DOPA in

- recurrent or metastatic medullary thyroid carcinoma. *Eur J Nucl Med Mol Imaging*. 2007;34:1604–1609.
30. Beheshti M, Pocher S, Vali R, et al. The value of  $^{18}\text{F}$ -DOPA PET-CT in patients with medullary thyroid carcinoma: comparison with  $^{18}\text{F}$ -FDG PET-CT. *Eur Radiol*. 2009;19:1425–1434.
  31. Marzola MC, Pelizzo MR, Ferdeghini M, et al. Dual PET/CT with  $^{18}\text{F}$ -DOPA and  $^{18}\text{F}$ -FDG in metastatic medullary thyroid carcinoma and rapidly increasing calcitonin levels: comparison with conventional imaging. *Eur J Surg Oncol*. 2010;36:414–421.
  32. Kloos RT, Eng C, Evans DB, et al. Medullary thyroid cancer: management guidelines of the American Thyroid Association. *Thyroid*. 2009;19:565–612.
  33. Neels OC, Koopmans KP, Jager PL, et al. Manipulation of [ $^{11}\text{C}$ ]-5-hydroxytryptophan and 6- $^{18}\text{F}$ fluoro-3,4-dihydroxy-L-phenylalanine accumulation in neuroendocrine tumor cells. *Cancer Res*. 2008;68:7183–7190.
  34. Orlefors H, Sundin A, Lu L, et al. Carbidopa pretreatment improves image interpretation and visualisation of carcinoid tumours with  $^{11}\text{C}$ -5-hydroxytryptophan positron emission tomography. *Eur J Nucl Med Mol Imaging*. 2006; 33:60–65.